Nonlinear interaction of proton whistler with kinetic Alfvén wave to study solar wind turbulence

R. Goyal, R. P. Sharma, M. L. Goldstein, and N. K. Dwivedi

Citation: Physics of Plasmas (1994-present) **20**, 122308 (2013); doi: 10.1063/1.4849457
View online: http://dx.doi.org/10.1063/1.4849457
View Table of Contents: http://scitation.aip.org/content/aip/journal/pop/20/12?ver=pdfcov
Published by the AIP Publishing

Nonlinear interaction of proton whistler with kinetic Alfvén wave to study solar wind turbulence

R. Goyal,[1,a)] R. P. Sharma,[1,b)] M. L. Goldstein,[2] and N. K. Dwivedi[3]
[1]*Centre for Energy Studies, Indian Institute of Technology, Delhi-110016, India*
[2]*NASA Goddard Space Flight Centre, Code 673, Greenbelt, Maryland 20771, USA*
[3]*Austrian Academy of Sciences, Space Research Institute, Schmiedlstrasse 6, 8042 Graz, Austria*

(Received 10 October 2013; accepted 3 December 2013; published online 17 December 2013)

This paper presents the nonlinear interaction between small but finite amplitude kinetic Alfvén wave (KAW) and proton whistler wave using two-fluid model in intermediate beta plasma, applicable to solar wind. The nonlinearity is introduced by modification in the background density. This change in density is attributed to the nonlinear ponderomotive force due to KAW. The solutions of the model equations, governing the nonlinear interaction (and its effect on the formation of localized structures), have been obtained using semi-analytical method in solar wind at 1AU. It is concluded that the KAW properties significantly affect the threshold field required for the filament formation and their critical size (for proton whistler). The magnetic and electric field power spectra have been obtained and their relevance with the recent observations of solar wind turbulence by *Cluster* spacecraft has been pointed out. © *2013 AIP Publishing LLC*. [http://dx.doi.org/10.1063/1.4849457]

I. INTRODUCTION

Solar wind is predominantly in turbulent state and is known to be a low density plasma.[1] Over the past decades, solar wind turbulence has been extensively studied both observationally and theoretically at the large scales where the Magnetohydrodynamic (MHD) approximation is valid.[2] In the dissipation range at scales much smaller than MHD scales, the nature of solar wind turbulence is still in debate.[1]

Solar wind fluctuations can be divided into three distinct regions[3,4] depending on the frequency and wave number. The first region corresponds to lower frequencies and consistent with k^{-1}, k being the wave number and this region consists of a flatter spectrum. The second region is having an index range from $k^{-3/2}$ to $k^{-5/3}$, which extends upto the ion/proton gyrofrequency. The usual MHD model describes the second part of fluctuations, which is characterized by fully developed turbulence. The latter part of the fluctuations incorporates turbulent interactions which are solely described by Alfvénic cascades.

The length scales exhibit a spectral break beyond the MHD regime and have spectral slope varying from −2 to −5.[4–6] Such a wide variation in turbulent spectrum can be attributed to kinetic Alfvén wave (KAWs),[7] the electromagnetic ion-cyclotron-Alfvén (EMICA) waves,[8,9] whistlers[10] or to a class of fluctuations, which come under the framework of the nonlinear Hall magnetohydrodynamics (H-MHD) and nonlinear electron-MHD (E-MHD) plasma models.[11]

Alfvénic MHD cascades[4–6] are not found after spectral break when observed in higher time resolutions and proton cyclotron damping is supposed to suppress these cascades. The power spectrum is observed, which seems to be consisting of damped magnetosonic and/or whistler waves. These waves are dispersive unlike Alfvén waves.[12] Electron motions get decoupled from ion motions due to fluctuations corresponding to high frequency regimes, ions become unmagnetized and can be considered to form a static neutralized background fluid. Although whistler wave propagation effects have significant role in EMHD turbulence, the linear wave dispersion relation does not play any role in the local spectral energy transfer process, contrary to the behavior seen in MHD turbulence mediated by Alfvén waves.[13]

Sahraoui *et al.*[14] have studied the relevance of various plasma modes including KAW and whistler to carry energy cascades in the solar wind down to electron scales. Also, there is a significant contribution by whistler turbulence to the "dispersion range" whose frequency spectrum is relatively steeper and is observed in solar wind.[10] Helios spacecraft detected the evidence of whistler waves in solar wind.[15–17] Various plasma systems incorporate vital role played by whistler waves in their turbulent cascades. These plasma systems may be exemplified as solar wind[18,19] and astrophysical plasmas.[20]

There is a change in the sense of polarization of whistler wave propagating in a plasma medium when its frequency matches the cross-over frequency. Due to this polarization reversal, a right-hand polarized electron whistler can be converted into left-hand polarized proton whistler.[21] Meyrand and Galtier[22] have studied the effect of left and right handed polarization on turbulent dynamics using their numerical simulation approach by introducing the effect of H-MHD. Proton whistlers are observed in the ionosphere[23] and are dispersed form of lightning impulses. These are detected as propagating left-handed polarized waves. At a wave frequency slightly below the proton gyrofrequency, the amplitude of these waves decreases sharply.[24] Some of the parameters in the ionosphere have been estimated by a number of workers using the observed characteristic features of proton whistlers.[23–26]

In the present work, proton whistler wave propagating in low frequency regime has been considered. First, we adopt a semi-analytical approach to study the formation of localized

[a)]Electronic mail: ravig.iitd@gmail.com
[b)]Electronic mail: rpsharma@ces.iitd.ac.in

structures of KAWs under paraxial approximation in intermediate – β plasma when the KAW intensity is having a Gaussian profile along x axis. We have studied the interaction of these localized structures of KAWs with low frequency proton whistler wave propagating through these filaments. The KAW and proton whistler localized structures are obtained along the direction of propagation using system of equations of KAW and low frequency proton whistler signals. The power spectra for both waves are estimated using the data so obtained for the solar wind. The paper is organised as follows.

In Sec. II, we give model equations of KAW in intermediate – β plasma and having x-z plane of propagation. Dynamics of weak proton whistler wave and it's interaction with KAW is given in Sec. III, and Sec. IV contains the summary and conclusions.

II. KINETIC ALFVÉN WAVE (KAW) DYNAMICS

With background magnetic field $\tilde{B}_0$ along z-axis in the magnetized plasma, finite amplitude KAW with low frequency is considered to be propagating in x-z plane. The KAW is derived following the standard method in the form of a dynamical equation using Maxwell's equations as follows.

The fluid velocities of electron and ion along their perpendicular directions are given by

$$\vec{v}_{e\perp} \approx \left(\frac{c}{B_0}\right)\vec{E}_x \times \hat{z}, \tag{1}$$

$$\vec{v}_{i\perp} \approx \left(\frac{c\omega_{ci}^2}{B_0\left(\omega_{ci}^2-\omega_0^2\right)}\right)\left(\vec{E}_x \times \hat{z}\right) + \left(\frac{c}{B_0}\right)\left(\frac{\omega_{ci}}{\omega_{ci}^2-\omega_0^2}\right)\frac{\partial \vec{E}_x}{\partial t}, \tag{2}$$

where ω_0 is the frequency of the KAW as pump wave, ω_{ci} being ion cyclotron frequency. $\vec{E}_x\left(\vec{E}_z\right)$ is $x(z)$-component of KAW electric field, and c is velocity of light in free space. The electron fluid velocity along parallel direction can be written in the form

$$\frac{\partial \vec{v}_{ez}}{\partial t} = -\frac{e\vec{E}_z}{m_e} - \frac{\hat{b}.\vec{\nabla}\mathrm{P}_e}{m_e n_e}, \tag{3}$$

where $m_e(m_i)$ is the mass of the electron (ion) and n_e is the modified electron density, and P_e is electron pressure. The KAW magnetic and electric fields are related by Faraday's law

$$\frac{\partial \tilde{B}_y}{\partial t} = c\frac{\partial \vec{E}_z}{\partial x} - c\frac{\partial \vec{E}_x}{\partial z}. \tag{4}$$

The nonlinear ponderomotive force of the KAW creates nonresonant density perturbation $\delta n_s(=n_e-n_0)$ by making use of which we derive the dynamical equation for the waves. n_0 is the background plasma density in the absence of waves. For this, the parallel component of Ampere's law is used, i.e., given by

$$\vec{\nabla} \times \vec{\mathrm{B}} = \frac{4\pi\vec{J}}{c}, \tag{5}$$

where $\vec{J} = -ne\vec{v}$ is total current density. Putting the values of $\vec{v}$ in component forms, the current density is written as

$$\vec{J} = \frac{n_e e c \omega_{ci}}{B_0\left(\omega_{ci}^2-\omega_0^2\right)}\frac{\partial \vec{E}_x}{\partial t} - n_e e v_{ez}. \tag{6}$$

Now, by inserting Eqs. (1) and (2) into the current density conservation equation $(\vec{\nabla}\cdot\vec{J}=0)$, we get

$$\frac{\partial \vec{E}_x}{\partial t} = -\left(1+\frac{1}{\omega_{ci}^2}\frac{\partial^2}{\partial t^2}\right)\frac{V_A^2}{c}\left(1-\frac{\delta n_s}{n_0}\right)\frac{\partial \tilde{B}_y}{\partial z}, \tag{7}$$

where $\delta n_s = n_e - n_0$ is the change in number density. The parallel electric field with its time derivative can be obtained using Eq. (3), equation of continuity and the parallel component of Ampere's law and is written as follows:

$$\frac{\partial \vec{E}_z}{\partial t} = \frac{\lambda_e^2}{c}\frac{\partial^3 \tilde{B}_y}{\partial x \partial t^2} - \frac{V_{Te}^2\lambda_e^2}{c}\frac{\partial^3 \tilde{B}_y}{\partial x \partial z^2}, \tag{8}$$

where $V_{Te}\left(=\sqrt{T_e/m_e}\right)$ is thermal speed of electrons and V_{Ti} $\left(=\sqrt{T_i/m_i}\right)$ is thermal speed of ions. $T_e(T_i)$ is the temperature of electron (ion), $\lambda_e\left(=\sqrt{c^2m_e/4\pi n_0 e^2}\right)$ defines the electron inertial length.

Using Eqs. (7) and (8) in the time derivative of Eq. (4), the equation for KAW with nonlinear dynamics is obtained as

$$\frac{\partial^2 B_y}{\partial t^2} = -\left(V_{Te}^2\lambda_e^2 + V_A^2\rho_i^2\right)\frac{\partial^4 B_y}{\partial x^2 \partial z^2} + V_A^2\left(1-\frac{\delta n_s}{n_0}\right)\frac{\partial^2 B_y}{\partial z^2} + \frac{V_A^2}{\omega_{ci}^2}\left(1-\frac{\delta n_s}{n_0}\right)\frac{\partial^4 B_y}{\partial t^2 \partial z^2}. \tag{9}$$

Here, ponderomotive force of the KAW plays its role due to which the background density is modified in intermediate-β plasma[27] and is given as follows:

$$\frac{\delta n_s}{n_0} = \phi\left(\tilde{B}\tilde{B}^*\right), \tag{10}$$

where $\phi\left(\tilde{B}\tilde{B}^*\right) = \exp\left(\gamma\tilde{B}\tilde{B}\right) - 1$, $\gamma = \left[(1-\alpha_0(1+\delta))/16\pi n_0 T\right]$ $\left(V_A^2 k_{0z}^2/\omega_0^2\right)$, $\alpha_0 = \omega_0^2/\omega_{ci}^2$, $\delta = m_e k_{0x}^2/m_i k_{0z}^2$, and $k_{0x}(k_{0z})$ is the wave vector perpendicular (parallel) to $\hat{z}B_0$.

Equation (9) is solved semi-analytically within paraxial approximation $(x \ll r_0 f_0)$.[28] Here, r_0 is the scale size of the pump wave, i.e., KAW in the transverse direction and f_0 is the beam width parameter, a dimensionless quantity. Substituting the envelope solution $B_y = \tilde{B}_0(x,z)e^{i(k_{0x}x+k_{0z}z-\omega_0 t)}$ into Eq. (9) and assuming $\partial_z\tilde{B}_0 \ll k_{0z}\tilde{B}_0$ and $\partial_x\tilde{B}_0 \gg k_{0x}\tilde{B}_0$, the nonlinear equation for KAW is written as

$$2ik_{0z}\left(1-\omega^2/\omega_{ci}^2\right)\frac{\partial \tilde{B}_0}{\partial z} - \frac{k_{0z}^2}{V_A^2}\left(V_{Te}^2\lambda_e^2 + V_A^2\rho_i^2\right)\frac{\partial^2 \tilde{B}_0}{\partial x^2} - k_{0z}^2\left(1-\omega^2/\omega_{ci}^2\right)\phi\left(\tilde{B}_0\tilde{B}_0^*\right)\tilde{B}_0 = 0, \tag{11}$$

where $\rho_i(=V_{Ti}/\omega_{ci})$ is ion gyroradius.

The solution for $\tilde{B}_0$ can be written as[29]

$$\begin{aligned}\tilde{B}_0 &= \tilde{A}_0(x)e^{ik_{0z}S_0(x,z)}\\ A_0^2 &= \frac{\tilde{B}_{00}^2}{f_0}\exp\left(\frac{-x_0^2}{r_0^2 f_0^2}\right)\\ S_0 &= \varsigma\frac{x^2}{2}+\phi_0\\ \varsigma &= a\frac{1}{f_0}\frac{df_0}{dz},\end{aligned} \tag{12}$$

where in Eq. (12), $a=[\{(\rho_i^2+\rho_s^2)k_{0z}^2\}^{-1}(1-\omega^2/\omega_{ci}^2)]$, $\rho_s(=c_s/\omega_{ci})$ is the ion sound radius at electron temperature, $c_s(=\sqrt{T_e/m_i})$ is the ion sound speed, and f_0 is governed by the differential equation

$$\frac{d^2f_0}{dz^2}=\frac{1}{a^2R_d^2f_0^3}-\frac{\gamma B_{00}^2}{ar_0^2f_0^2}e^{\frac{\gamma B_{00}^2}{f_0^2}}, \tag{13}$$

where $R_d=k_{0z}r_0^2$.

Equation (13) shows the propagation of KAW with normalized distance. The right hand side of Eq. (13) shows the competition between the diffraction and nonlinear terms. When these two terms balance each other, we get a self-trapping mode. In that case, no convergence or divergence of the wave takes place as it propagates (i.e., $f_0=1$) and hence we can calculate the value of critical magnetic field $\sim\tilde{B}_{00}(cr)$.

The plasma parameters for solar wind used in present study are as follows: $\beta_e\approx0.7$, $\beta_i\approx2.5$ are $B_0\approx6\times10^{-5}G$, $n_0\approx3\,\mathrm{cm}^{-3}$, $T_e=1.4\times10^5\mathrm{K}$, and $T_i=5.8\times10^5\mathrm{K}$. Using these values, the other parameters obtained: $V_A\approx7.5\times10^6\,\mathrm{cm/s}$, $V_{Te}\approx1.4\times10^8\,\mathrm{cm/s}$, $V_{Ti}\approx6.923\times10^6\,\mathrm{cm/s}$, $\omega_{ci}=0.574\,\mathrm{s}^{-1}$, $\lambda_e=3.07\times10^5\mathrm{cm}$, $\rho_i\approx1.204\times10^7\,\mathrm{cm}$, $\rho_s\approx5.9\times10^6\,\mathrm{cm}$, $a=4.6\times10^4$, $r_0=1.2\times10^{12}\,\mathrm{cm}$. For $\omega_0/\omega_{ci}=0.012$ and $k_{0x}\rho_s=0.009$; $\omega_0=0.007\,\mathrm{s}^{-1}$, $k_{0x}\approx1.66\times10^{-9}\,\mathrm{cm}^{-1}$, and $k_{0z}\approx3.47\times10^{-10}\,\mathrm{cm}^{-1}$. The critical value of the KAW field can be calculated for these parameters to be $\tilde{B}_{00}(Cr)=1.58\times10^{-9}\mathrm{G}$. The values of other parameter are: $\tilde{B}_{00}=2.63\times10^{-8}\mathrm{G}$, $R_d=5.00\times10^{14}\mathrm{cm}$, and $\gamma=5.02\times10^7$. $\tilde{B}_{00}$ is initial KAW field.

Keeping in view the plane wave front with initial conditions $df_0/dz=0$ and $f_0=1$ at $z=0$, Eq. (13) is solved for f_0, the beam width of KAW. Figure 1 shows the localization of KAW at different locations where it's magnetic intensity (normalized by $\tilde{B}_{00}^2$) distribution is plotted in solar wind region. Equation (13) explains the KAW localization. It can be narrated from Eq. (13) that the nonlinear term (i.e., the second term on the right-hand side) dominates when the critical value of magnetic field of KAW is dominated by its initial value and the value of beam width parameter f_0 goes on decreasing with the distance along propagation direction. But the diffraction term (i.e., the first term) starts dominating over the nonlinear term in the limit of small value of f_0. Therefore, f_0 starts increasing along direction of the propagation till the time it becomes large enough so that the nonlinear term becomes larger in comparison with the diffraction term. With the nonlinearity or nonlinear effects again dominating, there is again a decrease in f_0 untill domination of diffraction term f_0 starts diverging and the process repeats itself again. Hence, for KAW, there is certain minimum value of beam width f_0 and the main KAW intensity becomes very high in these small sized structures.

Figure 2 shows the KAW magnetic field power spectrum at $x=0$ and it is shown as $|B_k|^2$varying along k (where k is $|k|$). Figure 2 shows that in the initial range, the power spectrum has the index of $k^{-1.6}$, which resembles with Kolmogorov scaling law. After this, a breakpoint is observed in the spectrum with a steeper scaling of $k^{-2.3}$. This kind of spectrum is observed by Sahraoui *et al.*[30] They suggested that at the latter part of the spectrum, energy of the turbulence undergoes another dispersive cascade and is slightly damped. The typical $k^{-5/3}$ Kolmogorov form wave number spectrum indicates strong nonlinear couplings and quasi-

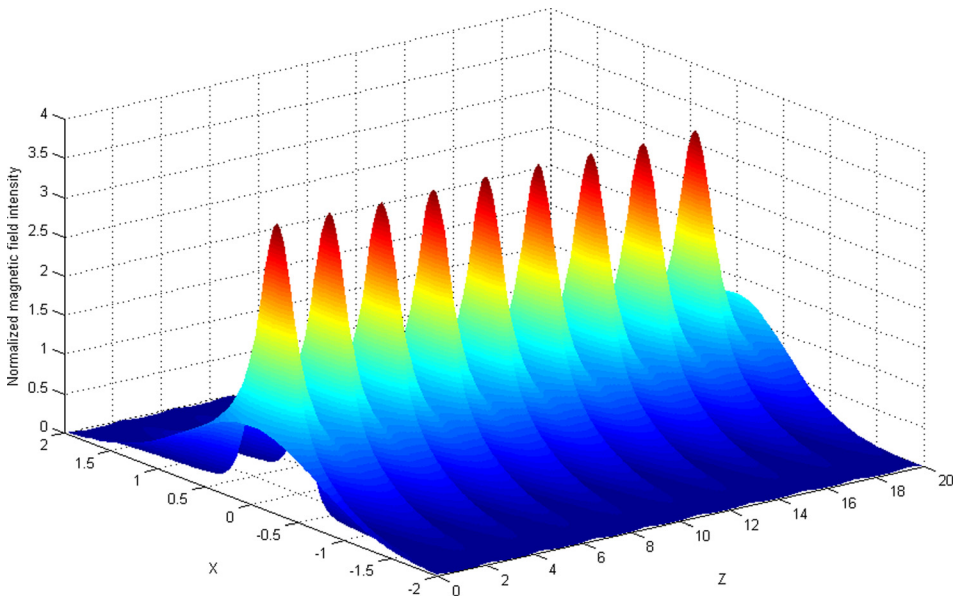

FIG. 1. The magnetic field intensity (normalized by$\tilde{B}_{00}^2$) of KAW varying with x and $\xi=z/R_d$ (denoted by z) defining the normalized distance of propagation.

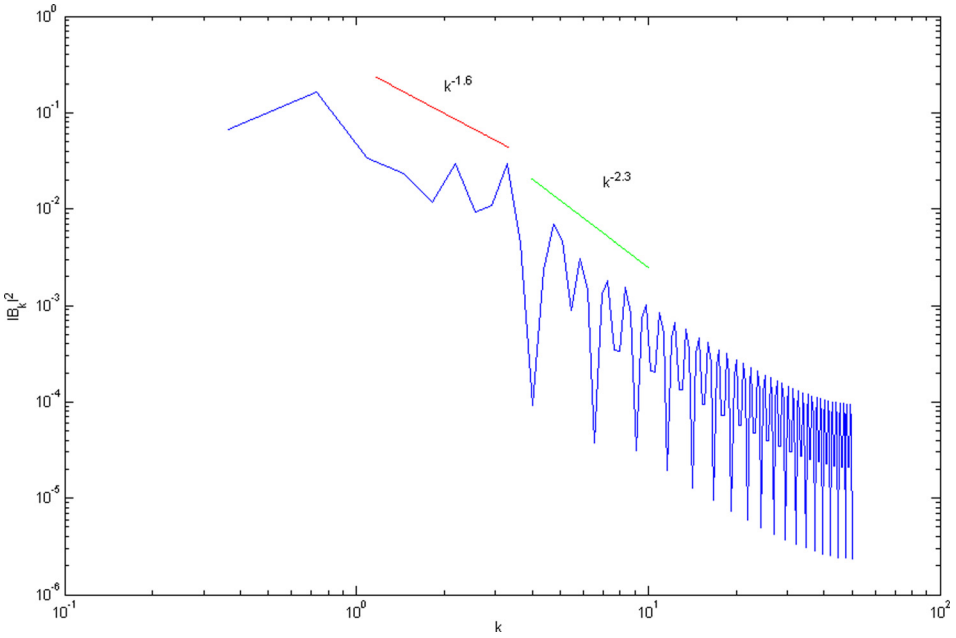

FIG. 2. Variation of normalized $|B_k|^2$ against k (where k is$|k|$) at $x = 0$ of the KAW. R_d^{-1} is normalization constant of k.

steady spectral transfer. So, the resultant power spectrum describing the magnetic field fluctuations is the probable indication of distribution of energy by nonlinear interactions among wave numbers of large and intermediate range.

In the present work, we have considered the modulation of weak proton whistler signal as a result of self-focussing and localization of KAW when proton whistler wave propagates through density channels produced by the KAW and due to which proton whistler amplitude gets regularly enhanced at the spots of narrow beam width. To explain this, we have described the KAW and proton whistler coupled system as given in Sec. III.

III. DYNAMICS OF PROTON WHISTLER WAVE

Here, the proton whistler wave is considered to be propagating along the z-direction, i.e., along the background magnetic field lines. For the field variations given by $e^{i\omega t}$, the wave equation can be given as

$$\nabla^2\vec{E} - \nabla(\nabla.\vec{E}) = -\frac{\omega^2}{c^2}\bar{\bar{\varepsilon}}.\vec{E}. \tag{14}$$

Here, $\bar{\bar{\varepsilon}}$ is the dielectric tensor.

In component form, the wave equation is written as follows:

$$\frac{\partial^2 E_x}{\partial z^2} - \frac{\partial}{\partial x}\left(\frac{\partial E_z}{\partial z}\right) = -\frac{\omega^2}{c^2}(\bar{\bar{\varepsilon}}.\vec{E})_x, \tag{15}$$

$$\frac{\partial^2 E_y}{\partial z^2} - \left(\frac{\partial^2 E_z}{\partial x^2}\right) = -\frac{\omega^2}{c^2}(\bar{\bar{\varepsilon}}.\vec{E})_y, \tag{16}$$

$$\frac{\partial^2 E_z}{\partial z^2} - \frac{\partial}{\partial z}\left(\frac{\partial E_x}{\partial y}\right) = -\frac{\omega^2}{c^2}(\bar{\bar{\varepsilon}}.\vec{E})_z. \tag{17}$$

The two coupled modes are denoted by left circularly polarized mode A_1 and right circularly polarized mode A_2 and these are given as follows:

$$A_1 = E_x + iE_y \tag{18}$$

and

$$A_2 = E_x - iE_y. \tag{19}$$

Using Eqs. (15) and (16), considering $\nabla.\vec{D} = 0$ where $\vec{D} = \bar{\bar{\varepsilon}}.\vec{E}$ and taking $\partial/\partial y = 0$, the dynamical equations for two coupled modes are written as

$$\frac{\partial^2 A_1}{\partial z^2} + \frac{1}{2}\frac{\partial^2 A_1}{\partial x^2} - \frac{1}{2}\frac{\partial^2 A_2}{\partial x^2} - i\frac{\partial^2 A_2}{\partial x \partial y} + \frac{\omega^2}{c^2}\varepsilon_{+0}A_1 = 0 \tag{20}$$

and

$$\frac{\partial^2 A_2}{\partial z^2} + \frac{1}{2}\frac{\partial^2 A_2}{\partial x^2} - \frac{1}{2}\frac{\partial^2 A_1}{\partial x^2} + \frac{\omega^2}{c^2}\varepsilon_{-0}A_2 = 0. \tag{21}$$

Here, in the present study, we are interested only in one model and hence on assuming $A_2 = 0$, Eq. (20) gives

$$\frac{\partial^2 A_1}{\partial z^2} + \frac{1}{2}\frac{\partial^2 A_1}{\partial x^2} + \frac{\omega^2}{c^2}\varepsilon_{+0}A_1 = 0, \tag{22}$$

where

$$\varepsilon_0 = 1 - \left(1 + \frac{\delta n_s}{n_0}\right)\left(\frac{\omega_p^2}{\omega^2}\right),$$

$$\varepsilon_{+0} = 1 - \left(1 + \frac{\delta n_s}{n_0}\right)\left[\frac{\omega_{pe}^2}{\omega(\omega + \omega_{ce})}\right] - \left(1 + \frac{\delta n_s}{n_0}\right)\left[\frac{\omega_{pi}^2}{\omega(\omega - \omega_{ci})}\right],$$

$$\varepsilon_{-0} = 1 - \left(1 + \frac{\delta n_s}{n_0}\right)\left[\frac{\omega_{pe}^2}{\omega(\omega - \omega_{ce})}\right] - \left(1 + \frac{\delta n_s}{n_0}\right)\left[\frac{\omega_{pi}^2}{\omega(\omega + \omega_{ci})}\right].$$

$\omega_{pe}(=\sqrt{4\pi n_0 e^2/m_e})$ is the electron plasma frequency and $\omega_{pi}(=\sqrt{4\pi n_0 e^2/m_i})$ is the ion plasma frequency, $\omega_{ce}(=eB_0/m_e c)$ is the electron gyrofrequency, ω_{ci} $(=eB_0/m_i c)$ being the ion gyrofrequency, ω is the frequency of proton whistler wave, and we are considering low frequency proton whistler mode, $\omega/\omega_{ci} \approx 0.1$' $\delta n_s = n_e - n_0$ (given in Eq. (10)).

We employ a plane wave solution in order to solve Eq. (22), which is given as

$$A_1 = Ae^{i(\omega t - k_+ z)}, \tag{23}$$

where $k_+ = \frac{\omega}{c}\varepsilon_{+00}^{1/2}$, ε_{+00} being the linear part of ε_{+0}, and A is the amplitude of complex nature.

Using above generalized plane wave solution in Eq. (22) and assuming $\partial_z A \ll k_+ A$, Eq. (22) is again written as

$$-2ik_+\frac{\partial A}{\partial z} + \frac{1}{2}\frac{\partial^2 A}{\partial x^2} + \frac{\omega^2}{c^2}\varepsilon_{+0}A - k_+^2 A = 0. \tag{24}$$

Now, Eq. (24) can be separated into real and imaginary parts by the introduction of additional factor eikonal. So, we can rewrite the form of A as

$$A = A_0(x)e^{-ik_+ S_+(x)}.$$

The real part of Eq. (24) can be written as

$$-2k_+^2 A_0^2\frac{\partial S_+}{\partial z} + \frac{A_0}{2}\left[\frac{\partial^2 A_0}{\partial x^2} - k_+^2 A_0\left(\frac{\partial S_+}{\partial x}\right)^2\right] + \frac{\omega^2}{c^2}\varepsilon_{+0}A_0^2 - k_+^2 A_0^2 = 0 \tag{25}$$

and the imaginary part is given by

$$-2k_+ A_0\left(\frac{\partial A_0}{\partial z}\right) + \frac{A_0}{2}\left[-2k_+\frac{\partial A_0}{\partial x}\frac{\partial S_+}{\partial x} - k_+ A_0\frac{\partial^2 S_+}{\partial x^2}\right] = 0. \tag{26}$$

Solutions of Eqs. (25) and (26) are written as follows:

$$A_0^2 = \frac{E_0^2}{f_+}e^{-x^2/r_+^2 f_+^2},$$
$$S_+ = \frac{x^2}{2}\beta(z) + \phi(z), \tag{27}$$
$$\beta(z) = \frac{2}{f_+}\frac{df_+}{dz}.$$

The variation of dimensionless beam width parameter f_+ for proton whistler signal is obtained by using Eq. (27) in Eq. (25) and equating the coefficient of x^2 on both sides as

$$\frac{d^2 f_+}{dz^2} = \frac{1}{4}\frac{r_0^4}{R_{dw}^2 r_w^4}\frac{1}{f_+^3} - \frac{f_+}{2}\frac{\gamma B_{00}^2}{r_0^2 f_0^2}e^{\frac{\gamma B_{00}^2}{f_0^2}}, \tag{28}$$

where $R_{dw} = k_+ r_w^2$. r_w is the scale size of the proton whistler wave in transverse direction. Now, considering f_+ having a plane wave front, Eq. (28) is solved with the initial conditions given by $df_+/dz = 0$ and $f_+ = 1$ at $z = 0$. The parameters used for proton whistler signal are $r_w = 2.4 \times 10^{12}$cm, $\omega = 0.057\text{s}^{-1}$, $k_+ = 8.185 \times 10^{-9}\text{cm}^{-1}$, $\omega_{pe} = 9.77 \times 10^4\text{s}^{-1}$, and $\omega_{pi} = 2.28 \times 10^3\text{s}^{-1}$.

It is clear from the right hand side of Eq. (28) that the value of f_+ depends on the diffraction (first) term and the nonlinear (second) term. In the absence of any nonlinearity, i.e., when second term on right hand side of Eq. (28) is zero, there is no convergence of proton whistler wave and its intensity would be continuously decreasing. However, in the presence of finite nonlinear term which is of equal magnitude as diffraction term, the proton whistler wave would neither

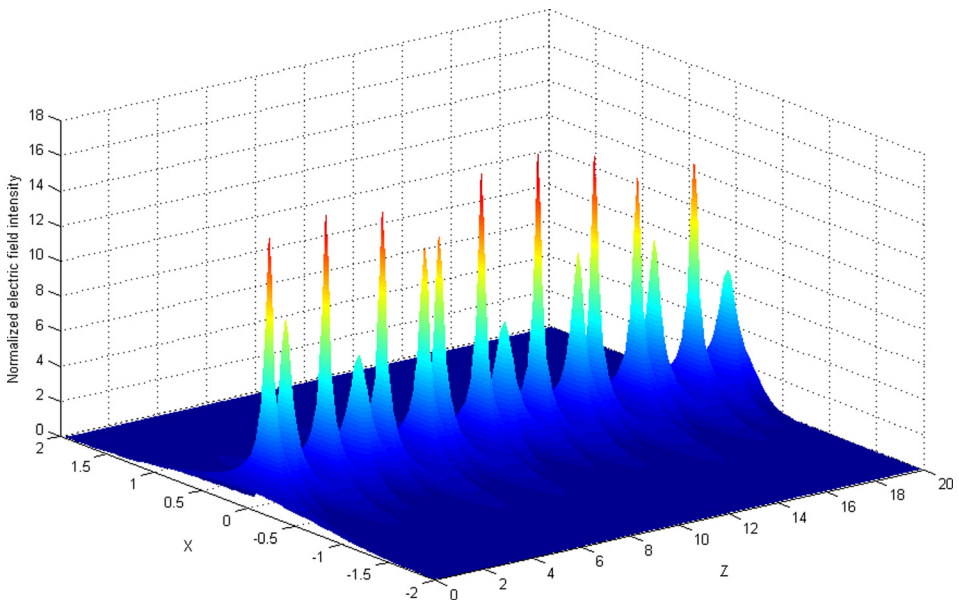

FIG. 3. The intensity of electric field (normalized by $\tilde{E}_{00}^2$) of the proton whistler wave varying with x and $\xi = z/R_{dw}$ (denoted by z), ξ being the normalized distance of propagation.

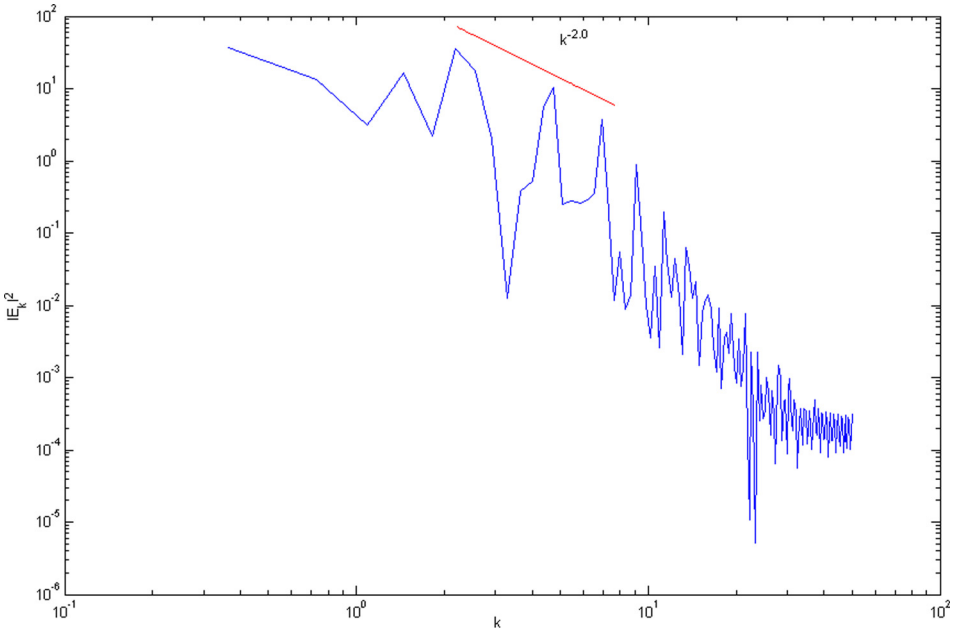

FIG. 4. Variation of normalized $|E_k|^2$ against k (where k is $|k|$) at $x = 0$ of the proton whistler wave. The normalization constant of k is R_{dw}^{-1}.

be converging nor diverging and $f_+ = 1$ and has perpetual amplitude signal. Equation (28) is solved numerically to study the modifications of weak proton whistler signal in inhomogeneous magnetized plasma (inhomogeneity introduced by the KAW) for typical parameters of KAW and proton whistler wave in solar wind region.

In Figure 3, we have shown the electric field intensity profile of proton whistler signal in solar wind plasmas. Equation (28) explains the localization of the proton whistler signal. Initially, when KAW gets localized, it creates the density channels due to modified electron density (ion density). The second term on the right hand side of Eq. (28) is coupled to the KAW due to the dependence of dielectric constant of proton whistler wave on KAW field intensity. The proton whistler amplitude gets periodically enhanced at narrow beam width points upon its propagation. The KAW self-focusing gives rise to nonlinear density filaments. When proton whistler signal propagates through these modified structures, its amplitude rises periodically. Thus, the electric field intensity profile of proton whistler signal is the net effect of diffraction and nonlinear terms. Therefore, the proton whistler signal becomes highly localized due to strong nonlinear interactions between KAW and weak proton whistler signal and the intensity of the proton whistler signal is maximum at points where f_+ is minimum.

Finally, the power spectrum of electric field of proton whistler wave is studied, which is shown in Figure 4 as $|E_k|^2$varying with k($|k|$). The power spectrum of electric field shows a scaling of k^{-2}. A number of authors[12,31–33] have studied the whistler spectra. In the present study, we have described the difference in proton whistler spectrum, which may be characterized to its nonlinear coupling with KAW when KAW generates nonlinear density filaments. The short scale turbulence generation may be described by this process. We have also described the turbulence spectra and magnetic field fluctuations of KAW created by KAW itself. The pertinency of the study with the observations[2,30] is also pointed out.

If we look at Figs. 2 and 4, we observe spectra with strong oscillations. We have developed a semi-analytical model in the paraxial regime in which the wave front of the pump wave is considered to be Gaussian. This model gives some approximate solutions; and therefore, we observed such a strong oscillation in the spectra. If we compare with the solar wind, we do not see such oscillations. In Fig. 4, we have observed a much steeper slope in the second part of the power spectrum, this type of spectrum in the later part might be due to the limitation of our model and we could not find any observational evidence of such type of spectrum. For more accurate solution and for getting realistic spectra, one has to perform the numerical simulation for non-paraxial regime. We shall do it in our future work and we are expecting that the strong oscillations are supposed to die down to some extent. Definitely, we will get much better spectral slope in the second part of the spectrum by doing numerical simulation (in non paraxial regime) of the present model.

IV. SUMMARY AND CONCLUSION

The localization of large amplitude kinetic Alfvén waves at oblique incidence to the ambient magnetic field in intermediate-β plasmas applicable to solar wind has been investigated in the present study. The background electron/ion density gets modified as a consequence of ponderomotive force which leads to KAW localization. The KAW while propagating through plasma, gets self focused and generates density filaments in the plasma and these density filaments modulate the weak proton whistler signal when it is made to pass through these filaments due to which the beam width of the signal gets narrower periodically along the propagation direction and the amplitude of the proton whistler wave gets enhanced at the spots where beam width is compressed. The intensity profiles of KAW and proton whistler signal have been described in the results. The magnetic power spectrum of KAW having a scaling $k^{-1.6}$ in the initial range of the spectrum has been shown in the results and a

second steeper spectrum is shown with a scaling of $k^{-2.3}$ in the latter part. The electric power spectrum of proton whistler wave has a scaling of k^{-2}. The similar kinds of spectra have been recently observed by Saharoui *et al.*[30] Although recent observations predict the evidence of the dominance of KAW at sub-ion scales and proton kinetic scales,[34] Perri *et al.*[35] observed the existence of a cascade of magnetic energy down to the smallest scales (electron scale), which is attributed to KAW spectrum and are small current sheets and discontinuities. In this way, it is worth to say that the KAW/whistler mode can carry the turbulence cascade down to electron scales. At $\omega \approx \omega_{ci}$, the resonance occurs for proton whistler and KAW imparts maximum of its energy to proton whistler wave. This proton whistler wave through mode coupling may impart its energy to the whistler mode. So, the present model shows that the nature of small scale turbulence can be described while both modes (KAW as well as proton whistler) are present in the wave dynamics simultaneously.

ACKNOWLEDGMENTS

This work was partially supported by DST (India) and ISRO (India) under RESPOND program.

[1]D. Verscharen, E. Marsch, U. Motschmann, and J. Müller, Phys. Plasmas **19**, 022305 (2012).
[2]F. Sahraoui, M. L. Goldstein, G. Belmont, P. Canu, and L. Rezeau, Phys. Rev. Lett. **105**, 1311012010).
[3]M. L. Goldstein, D. A. Roberts, and W. H. Matthaeus, Astron. Astrophys. **33**, 283 (1995).
[4]R. J. Leamon, N. F. Ness, C. W. Smith, and H. K. Wong, AIP Conf. Proc. **471**, 469 (1999).
[5]C. W. Smith, W. H. Matthaeus, and N. F. Ness, in *Proc. 21st Int. Conf. Cosmic Rays Graphics Services, Northfield* (1990), Vol. 5, p. 280.
[6]M. L. Goldstein, D. A. Roberts, and C. A. Fitch, J. Geophys. Res. **99**, 11519, doi:10.1029/94JA00789 (1994).
[7]A. Hasegawa and L. Chen, Phys. Rev. Lett. **36**, 23 (1976).
[8]J. J. Podesta, Sol. Phys. **286**, 529 (2013).
[9]C. S. Wu and P. H. Yoon, Phys. Rev. Lett. **99**, 075001 (2007).
[10]S. P. Gary, S. Saito, and H. Li, Geophys. Res. Lett. **35**, L02104, doi:10.1029/2007GL032327 (2008).
[11]D. Shaikh and P. K. Shukla, Phys. Rev. Lett. **102**, 045004 (2009).
[12]O. Stawicki, S. P. Gary, and H. Li, J. Geophys. Res. **106**, 8273, doi:10.1029/2000JA000446 (2001).
[13]S. Galtier and A. Bhattacharjee, Phys. Plasmas **10**, 3065 (2003).
[14]F. Sahraoui, G. Belmont, and M. L. Goldstein, Astrophys. J. **748**, 100 (2012).
[15]F. M. Neubauer, G. Musmann, and G. Dehmel, J. Geophys. Res. **82**, 3201, doi:10.1029/JA082i022p03201 (1977).
[16]F. M. Neubauer, H. J. Beinroth, H. Bamstorf, and G. Dehmel, J. Geophys. Res. **42**, 599 (1977).
[17]K. U. Denskat, H. J. Beinroth and F. M. Neubauer, J. Geophys. Res. **54**, 60 (1983).
[18]*Eur. Space Agency Spec. Publ. ESA SP-641*, edited by C. Salem, S. D. Bale, and M. Maksimovic (2007).
[19]S. Saito, S. P. Gary, H. Li, and Y. Narita, Phys. Plasmas **15**, 102305 (2008).
[20]I. Roth, Planet. Space Sci. **55**, 2319 (2007).
[21]A. K. Singh, Abhay K. Singh, D. K. Singh, and R. P. Singh, J. Atmos. Sol. Terr. Phys. **60**, 551 (1998).
[22]R. Meyrand and S. Galtier, Phys. Rev. Lett. **109**, 194501 (2012).
[23]D. A. Gurnett, S. D. Shawhan, N. M. Brice, and R. L. Smith, J. Geophys. Res. **70**, 7 (1965).
[24]D. A. Gurnett and N. M. Brice, J. Geophys. Res. **71**, 15 (1966).
[25]S. D. Shawhan and D. A. Gurnett, J. Geophys. Res. **71**, 1 (1966).
[26]D. A. Gurnett and S. D. Shawhan, J. Geophys. Res. **71**, 3 (1966).
[27]S. Kumar, R. P. Sharma, and H. D. Singh, Phys. Plasmas **16**, 072903 (2009).
[28]S. A. Akhmanov, A. P. Sukhorukov, and R. V. Khokhlov, Sov. Phys. Usp. **10**, 609 (1968).
[29]A. Shukla and R. P. Sharma, J. Atmos. Sol.-Terr. Phys. **64**, 661 (2002).
[30]F. Sahraoui, M. L. Goldstein, P. Robert, and Yu. V. Khotyaintsev, Phys. Rev. Lett. **102**, 231102 (2009).
[31]S. Galtier, J. Plasma Phys. **72**, 721 (2006).
[32]S. P. Gary and C. W. Smith, J. Geophys. Res. **114**, A12105, doi:10.1029/2009JA014525 (2009).
[33]S. Saito, S. P. Gary, H. Li, and Y. Narita, Phys. Plasmas **17**, 122316 (2010).
[34]Y. Voitenko and V. Peirrard, Sol. Phys. **288**, 369 (2013).
[35]S. Perri, M. L. Goldstein, J. C. Dorelli, and F. Sahraoui, Phys. Rev. Lett. **109**, 191101 (2012).